Ballistic Contributions to Heat-Pulse Propagation in the TFTR Tokamak

E. D. Fredrickson, K. McGuire, A. Cavallo, R. Budny, A. Janos, D. Monticello, Y. Nagayama, W. Park, G. Taylor, and M. C. Zarnstorff

Princeton Plasma Physics Laboratory, Princeton University, Princeton, New Jersey 08543

(Received 9 May 1990)

Measurements on the TFTR tokamak of the electron-temperature-profile evolution and soft-x-ray emissivity on a fast (10-μsec) time scale during a sawtooth crash show that significant heat is deposited beyond the mixing (or reconnection) radius within 200 μsec following a sawtooth crash. This extended region in which electron heat is redistributed during the sawtooth crash substantially complicates the determination of heat transport properties from the subsequent heat-pulse propagation. It is shown that the relaxation of this *extended* perturbation is consistent with the power-balance estimates of the local thermal diffusivity.

PACS numbers: 52.50.Gj, 52.55.Fa

The radial propagation of sawtooth-induced heat pulses has long been used to study thermal transport in tokamaks.[1-3] In part, this work was motivated by the "Kadomtsev model"[4] of the sawtooth crash where the electron heat was redistributed through a reconnection of the helical flux within the reconnection (or mixing) radius r_m, and no heat was deposited beyond that radius. Thus, the evolution of the electron temperature in the region exterior to the mixing radius would be governed completely by diffusion. This model was consistent with the experimental data that was available at that time, and opened up the possibility of directly measuring the local electron thermal transport coefficient χ_e. Subsequently, the Kadomtsev model of the sawtooth crash has come into question,[5-7] but the assumption that no heat is deposited beyond the reconnection radius is still fundamental to all perturbative heat-pulse-propagation analysis methods. (In this paper, "heat-pulse propagation" refers to the relaxation of the temperature perturbation following the sawtooth crash.)

A number of simple methods to determine the local thermal diffusivity based on the evolution of the heat pulse were derived,[2,3,8,9] with the assumption that the evolution of the temperature profile outside the mixing radius was governed by a diffusive process with a time-independent χ_e. The derivations are well documented in Refs. 1-3, 8, and 9, and will not be reproduced here. All derivations assume that χ_e was not time dependent, and that heat was not directly deposited outside the mixing radius (for the time-to-peak method, the method was only valid for $r > 1.4r_m$). The thermal diffusivities χ^{HP}'s derived by these methods are, in many cases, much larger (3-10 times) than the thermal diffusivity derived from power balance, χ^{PB}.[3,9] Further, different perturbation analysis methods, used on the same data, often give different answers. For the example discussed below, χ^{HP} is 6 m^2/sec using the simple time-to-peak method,[2,3] 12 m^2/sec with the extended time-to-peak method,[9] and 5 and 21 m^2/sec, respectively, using the phase and amplitude Fourier-analysis methods.[3,8] In the region of interest the power-balance χ_e was only 1.5 m^2/sec. When applied to heat-pulse data simulated with the experimental density profile and the power-balance χ_e profile, the extended time-to-peak and Fourier-transform methods give the local χ_e to within 10%. The simple time-to-peak method applied to the simulated data underestimates the local χ_e by a factor of 2, as expected, due to the strong gradient in $n\chi_e$.[3,9] Many models have been proposed to explain this discrepancy, including heat pinches,[3] temperature or temperature-gradient dependences in χ_e,[3] off-diagonal terms in the transport matrix,[10-12] or a strong enhancement of χ_e near r_m for a short time following the sawtooth crash (e.g., due to magnetic turbulence).[3,13]

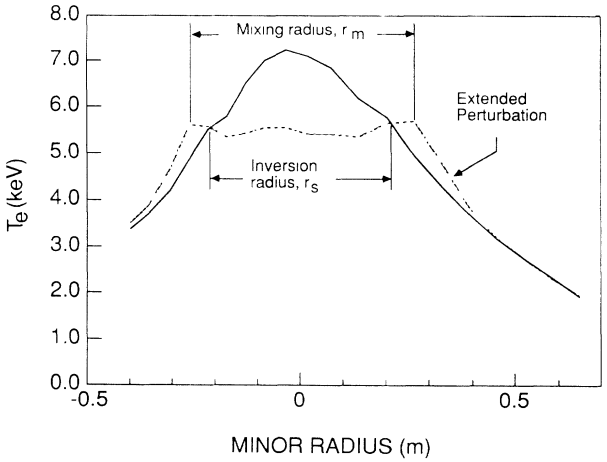

FIG. 1. Profiles of the electron temperature before (solid line) and 200 μsec after (dashed line) a sawtooth crash (the same as in Fig. 2). [The parameters for this shot were $I_p = 1.7$ MA, $q(a) = 4.4$, neutral-beam-injection power = 19 MW, $a = 0.8$ m, $R = 2.45$ m, and $B_T = 4.7$ T.]

Fast (10-μsec) electron-cyclotron-emission (ECE) measurements of the electron temperature profile in TFTR have been used to study the sawtooth crash mechanism as well as the propagation of the resulting heat pulse. Two features are observed in these fast data that would not be apparent with slower diagnostics. The first is the "ballistic" response where, in some cases, heat actually is deposited well beyond the reconnection radius on a very short time scale, i.e., within ~ 200 μsec following the sawtooth crash (Fig. 1). The second is the presence of a helical distortion outside the $q=1$ surface during the final phase of the sawtooth precursor. The measured electron temperature (and presumably the flux surfaces) shows a helical distortion which is seen to extend up to 0.15 m beyond the mixing radius of 0.28 m (Fig. 2). The distortion is poloidally asymmetric, having a very small amplitude on the high-field side of the machine. This bulging of the flux surfaces has only been seen on moderately-high-β_T plasmas, $\sim 1\%$ on axis, to date, but the deposition of heat beyond r_m has been observed even in Ohmic plasmas. The example chosen for study in this paper is a 1.7-MA, $q(a)=4.4$ plasma with 19 MW of neutral-beam-heating power.

Sawtooth crashes on approximately twenty plasmas have been studied in detail. These shots have covered a wide range of conditions ranging from Ohmically heated to neutral-beam-heated plasmas with up to 19 MW of beam power. While extensive documentation of this effect has been done only on TFTR, that it is observed here calls into question the validity of *any* sawtooth-induced heat-pulse analysis where the initial perturbation cannot be accurately determined. The poloidally symmetric redistribution of heat out to 0.15 m beyond the reconnection radius in less than 200 μsec has been observed down to β_T of $\sim 0.05\%$ in low-density, Ohmic plasmas. The extended perturbation is weaker in similar, but higher-density, lower-Z_{eff} plasmas. As a stronger extended perturbation would result in faster heat-pulse propagation, this result suggests that the density scaling of χ^{HP} observed on TFTR [14] and the scaling of χ^{HP} with Z_{eff} reported on JET [15] are a scaling of the extent of the extended perturbation.

Simulations of the heat-pulse propagation that do not take account of the extended perturbation at the sawtooth crash, using the χ_e derived from power balance (calculated with the time-dependent transport analysis code, TRANSP,[16] and averaged in time over the sawtooth period) predict a much slower rate of rise of the heat pulse near the mixing radius (Fig. 3). Similarly, simulations with an enhanced χ_e chosen to be 5 times the power-balance value, so that the simulated and experimental heat pulses had a similar time to peak at $r=0.65$ m, also did not have a fast enough rate of rise just outside the mixing radius (Fig. 4). Simulations with the local χ_e transiently enhanced following the crash can qualitatively reproduce the heat-pulse evolution in the region outside the mixing radius (Figs. 5 and 6). The time and spatial dependence of χ_e (in m^2/sec) used in the simulation was

$$\chi_e(r,t)=[0.3+3.8(r/a)^2] \times e^{1.1(r/a)^2}(1+150e^{-t/\tau-9.6(r/a)^2}), \quad (1)$$

where $\tau=1$ msec. This relatively simple model accurately reproduces the experimental data in the heat-pulse propagation region and thus illustrates several important features of the expected enhancement in $\chi(r,t)$. The required increase in the electron thermal diffusivity is about a factor of 40 immediately outside the mixing radius for a period of about 1 msec following the sawtooth

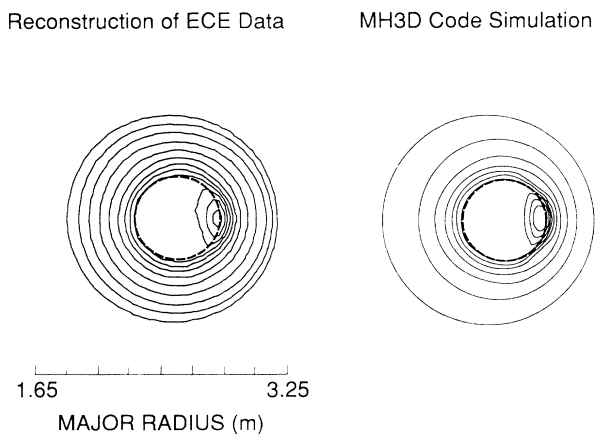

FIG. 2. Contours of constant electron temperature just prior to the sawtooth crash for shot No. 30904 and from the MH3D simulation for similar plasma parameters. The dashed circle represents the location of the equilibrium $q=1$ surface.

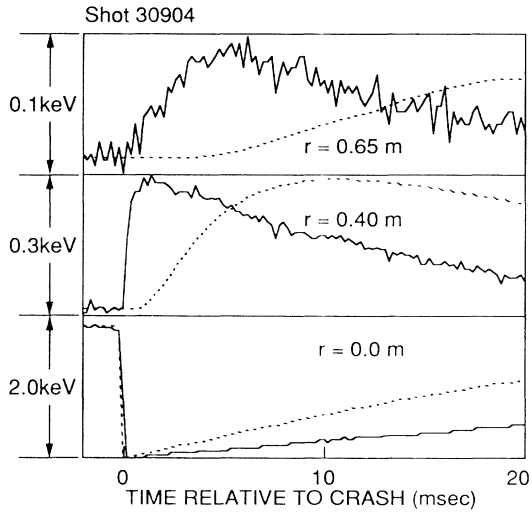

FIG. 3. Comparison of heat-pulse data from ECE emission (solid lines) to simulated heat pulses (dotted lines) where the power-balance profile has been used, $\chi(r)=[0.3+3.8\times(r/a)^2]e^{1.1(r/a)^2}$ m^2/sec.

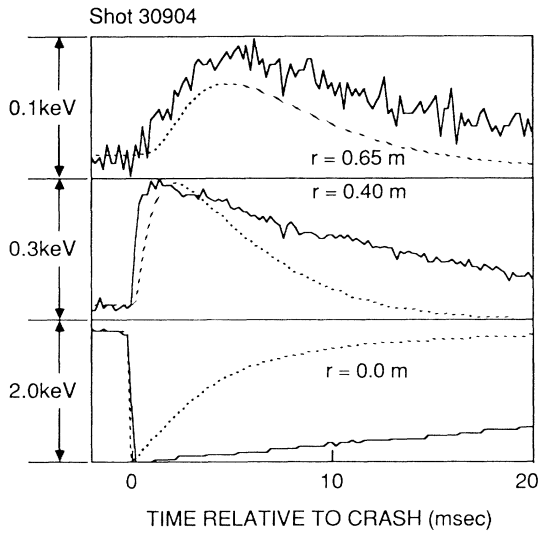

FIG. 4. Comparison of heat-pulse data (from ECE emission) and simulated data using $5\chi(r)$ as used in Fig. 3.

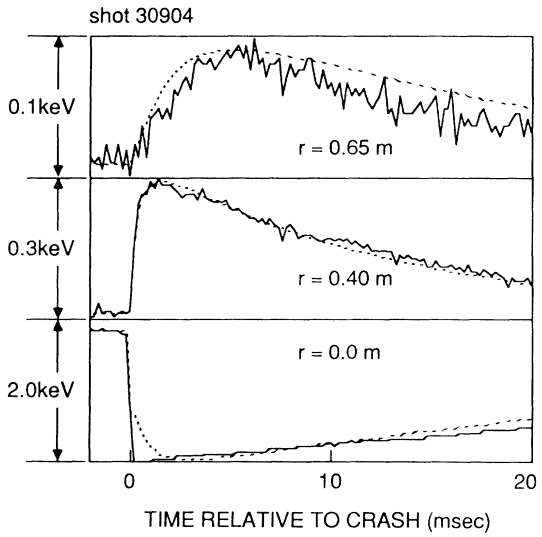

FIG. 5. Simulation of the heat-pulse propagation where the thermal diffusivity (in m^2/sec) is enhanced as in Eq. (1); the dimensionless density profile is $n_e(r)=e^{-1.1(r/a)^2}$, and $\tau=1$ msec.

crash. A likely explanation for this enhancement in transport would be stochastization of the flux surfaces for a short time following the sawtooth crash.[3,17,18]

Of particular importance is that with this model, after 1-2 msec following the sawtooth crash, the thermal diffusivity in the heat-pulse propagation region is hardly perturbed, and the perturbation as set up with the transiently enhanced χ_e relaxes with the power-balance χ_e. As described above, though, the propagation of the heat pulse, as analyzed with the time-to-peak or extended time-to-peak method, is faster than expected from the power-balance calculation of χ_e.

Numerical simulations of a sawtooth crash with the MH3D code[19] have predicted the presence of the helical bulge in the flux surfaces beyond[20,21] r_m (Fig. 2). (The $m=1$, $n=1$ helical nature of the equilibrium during the sawtooth precursor phase has been discussed in previous papers on sawtooth simulations.[22-24]) This comes about through the inclusion of nonlinear finite-pressure (or β) modifications of the $m=1$ sawtooth precursor mode, which extend the eigenfunction beyond r_m. The numerical simulations show a similar amplitude of perturbation to the experiment, including the poloidally asymmetric character of the perturbation; i.e., experimentally and in the simulation the perturbation is much smaller on the high-field side. In the present example this feature is measurable up to $\sim$0.15 m beyond the mixing radius before the amplitude drops below the noise level. It is only observable during the actual crash phase, but in other cases has been measurable for up to 1 msec before the sawtooth crash. From a careful examination of the phases of the in/out (ECE) and up/down (soft-x-ray) signals it is determined to be helical in nature, coincident with the location of the $m=1$ island x point. This evidence that the magnetic perturbation can extend well beyond the mixing radius, and with the poloidal asymmetry in the amplitude, supports the conjecture that the magnetic field becomes stochastic in that region immediately following the sawtooth crash. Indeed, the MH3D code simulation shows a stochastic region extending from the mixing radius to the $q=2$ surface (from $r=0.28$ to 0.58 m). However, the code was run with a value of S (the ratio of the resistive to Alfvén times) smaller than in the experiment ($\sim 10^5$ vs $\sim 10^9$ for the experiment) for speed of computation: Thus the actual stochastic region in the experiment may be somewhat smaller.

In summary, significant progress has been made in resolving the long-standing mystery of the anomalously rapid propagation of sawtooth-induced heat pulses on TFTR. Contrary to previous assumptions made in the studies of sawtooth-induced heat-pulse propagation, heat is seen to be deposited well beyond the mixing radius on a short time scale [$\leq 50\,\mu$sec with $(m,n)=(1,1)$ struc-

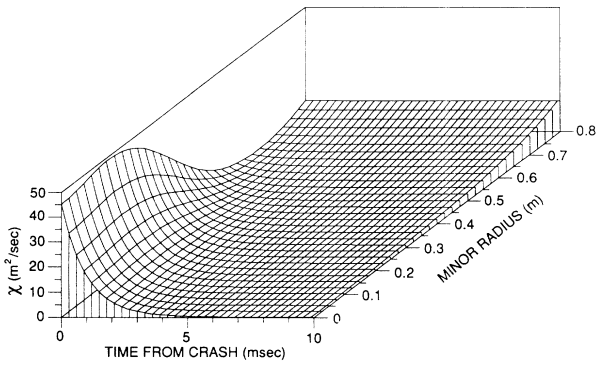

FIG. 6. The thermal diffusivity as used in Fig. 5.

ture, $\leq 200\,\mu$sec axisymmetrical] following the sawtooth crash. As the evolution of the electron temperature profile in this region is no longer completely governed by a time-independent χ_e, the present methods of analyzing heat-pulse propagation are not applicable on TFTR. Simulations suggest that the extended perturbation relaxes on a time scale consistent with the equilibrium power-balance value of χ_e, at least for the high-auxiliary-heating-power cases studied. Other effects which have recently been invoked in the study of heat-pulse propagation[10-12] may still be important in understanding transient transport phenomena, but great care must be exercised in their application to the analysis of sawtooth-induced heat-pulse propagation. The discovery that heat is transported beyond the mixing radius during the sawtooth crash shows that the physics of sawtooth crashes is richer than previously assumed.

The authors would like to thank W. Stodiek and J. Callen for many useful discussions and suggestions. This work was supported by U.S. DOE Contract No. DE-AC02-76CH0-3073.

[1]J. D. Callen and G. L. Jahns, Phys. Rev. Lett. **38**, 971 (1977).

[2]M. Soler and J. D. Callen, Nucl. Fusion **19**, 703 (1979).

[3]E. D. Fredrickson, J. D. Callen, K. M. McGuire, J. D. Bell, R. J. Colchin, P. C. Efthimion, K. W. Hill, R. Izzo, D. R. Mikkelsen, D. A. Monticello, V. Paré, G. Taylor, and M. Zarnstorff, Nucl. Fusion **26**, 849 (1986).

[4]B. B. Kadomtsev, Fiz. Plazmy **1**, 710 (1975) [Sov. J. Plasma Phys. **1**, 389 (1975)].

[5]K. M. McGuire *et al.*, in *Proceedings of the Eleventh International Conference on Plasma Physics and Controlled Nuclear Fusion Research, Kyoto, Japan, 1986,* edited by J. W. Weil and M. Demir (IAEA, Vienna, 1987), Vol. I, p. 421.

[6]H. Soltwisch and W. Stodiek, in *Proceedings of the Eleventh International Conference on Plasma Physics and Controlled Nuclear Fusion Research* (Ref. 5), Vol. I, p. 263.

[7]M. F. F. Nave and J. Wesson, Nucl. Fusion **28**, 297 (1988).

[8]G. L. Jahns, S. K. Wong, R. Prater, S. H. Lin, and S. Ejima, Nucl. Fusion **26**, 226 (1986).

[9]N. J. Lopes Cardozo, B. J. D. Tubbing, F. Tibone, and A. Taroni, Nucl. Fusion **28**, 1173 (1988).

[10]K. W. Gentle, Phys. Fluids **31**, 1105 (1988).

[11]M. Hossain, M. Kress, P. N. Hu, A. A. Blank, and H. Grad, Phys. Rev. Lett. **58**, 487 (1987).

[12]C. M. Bishop and J. W. Conner, Plasma Phys. Controlled Fusion **32**, 203 (1990).

[13]K. M. McGuire *et al.*, Plasma Phys. Controlled Fusion **30**, 1391 (1988).

[14]R. J. Goldston *et al.*, in *Proceedings of the Fifteenth European Conference on Controlled Fusion and Plasma Heating Dubrovnik, Yugoslavia, 1988,* edited by N. Cindro, R. Caplar, and J. Jacquinot (European Physical Society, Petit-Lancy, 1988).

[15]N. J. Lopes Cardozo and J. C. M. de Haas, Nucl. Fusion **30**, 521 (1990).

[16]R. J. Goldston, in *Physics of Plasma Close to Thermonuclear Conditions,* Proceedings of the Course, Varenna, 1979 (Commission of the European Communities, Brussels, 1980), Vol. 1, p. 19.

[17]C. Mercier, Fiz. Plazmy **9**, 132 (1983) [Sov. J. Plasma Phys. **9**, 82 (1983)].

[18]A. J. Lichtenberg, Nucl. Fusion **20**, 1277 (1984).

[19]W. Park and D. Monticello, Princeton Plasma Physics Laboratory Report No. PPPL-2601, 1989 [Nucl. Fusion (to be published)].

[20]W. Park, D. A. Monticello, E. D. Fredrickson, and K. M. McGuire, Princeton Plasma Physics Laboratory Report No. PPPL-2715, 1990 (to be published).

[21]W. Park, D. A. Monticello, E. D. Fredrickson, and K. M. McGuire, IAEA Report No. IAEA-CN-53/D-2-5, 1990 (to be published).

[22]B. V. Waddel, M. N. Rosenbluth, D. A. Monticello, and R. B. White, Nucl. Fusion **16**, 528 (1976).

[23]R. G. Kleva, J. F. Drake, and R. E. Denton, Phys. Fluids **30**, 2119 (1987).

[24]M. L. Theobald, D. Montgomery, and G. D. Doolen, Phys. Fluids B **1**, 766 (1989).